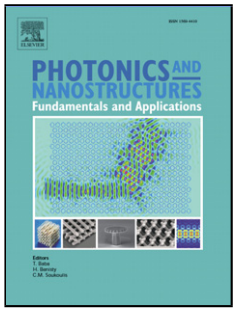

Title: Enhanced geometries of macroporous silicon photonic crystals for optical gas sensing applications

Authors: D. Cardador, D. Vega, D. Segura, T. Trifonov, A. Rodríguez

PII: S1569-4410(16)30102-X
DOI: http://dx.doi.org/doi:10.1016/j.photonics.2017.04.005
Reference: PNFA 590

To appear in: *Photonics and Nanostructures – Fundamentals and Applications*

Received date: 14-11-2016
Revised date: 21-3-2017
Accepted date: 18-4-2017

Please cite this article as: D.Cardador, D.Vega, D.Segura, T.Trifonov, A.Rodríguez, Enhanced geometries of macroporous silicon photonic crystals for optical gas sensing applications, Photonics and Nanostructures - Fundamentals and Applicationshttp://dx.doi.org/10.1016/j.photonics.2017.04.005

Enhanced geometries of macroporous silicon photonic crystals for optical gas sensing applications

D. CARDADOR[1], D. VEGA[1], D.SEGURA[1], T.TRIFONOV[2] AND A. RODRÍGUEZ[1]

[1]*Micro i Nanotecnologies, Departament d'Enginyeria Electrònica, Universitat Politècnica de Catalunya, C/Jordi Girona, 31, 08031, Barcelona, Spain.* - E-mail: david.cardador@upc.edu. Tel: +34 93 401 67 66.
[2]*Center for Research in NanoEngineering, CrNE—Universitat Politècnica de Catalunya, UPC, Barcelona 08028, Spain*

Highlights

- 3-d Photonic Crystals based on macroporous silicon with a cavity inserted in the middle of the structure have been explored to find an optimum Q-factor of their transmission peak.
- The shape optimization involved adjusting the pores' tail length and modifying the number of periods in the modulated section.
- It is demonstrated an increasing of more than an order of magnitude in the Q-factor of the transmitted peaks.
- The device response to CO_2 has been studied and has been found that for the optimized PhC structure, a large variation of 70% in transmitted peak amplitude can be obtained with a sensitivity about $0.8\ \%/c_{\%}$.
- The conclusion driven is that such PhCs are suitable for the detection of strong absorbing gases by non-dispersive infrared spectroscopy.

ABSTRACT

A macroporous silicon photonic crystal is designed and optimized theoretically for its use in gas sensing applications and IR optical filters. Light impinges perpendicularly onto the sample surface (vertical propagation) so a three-dimensional (3d) structure is used. For gas sensing, a sharp resonance is desired in order to isolate an absorption line of the gas of interest. The high Q-factors needed mandate the use of a plane defect inside the PhC to give rise to a resonant mode inside the bandgap tuned to the gas absorption line. Furthermore to allow gas passage through the device, an open membrane is required. This can affect the mechanical resilience. To improve the strength of the photonic crystal the pores are extended after the "active" 3d part. The number of modulations, and the extension length have been optimized to obtain the largest Q-factor with reasonable transmitted power. These proposed structures have been experimentally performed, probing an enhancement of almost an order of magnitude in the Q-factor in respect with the basic case. Simulations considering CO_2 have been performed showing that the proposed structures are promising as precise optical gas sensors.

1. INTRODUCTION

Photonic crystals (PhCs) exhibit photonic bandgaps (PBGs) in their optical spectra [1], [2], because of the periodical modulation of their refractive index. This feature allows creating resonating cavities, and thus PhCs can be used to create IR filters and devices for the optical detection of gases [3], [4]. These cavities are created by placing defects in the periodical structure of the PhC[5]. The detection can be then performed by directly monitoring the absorption of light, or by measuring a frequency shift of the peak. The direct measure method is based on the Beer-Lambert law, which states that the intensity absorption is an exponential function of substance concentration and optical length [6]. Gases, in particular, have strong optical absorption bands at specific wavelengths unique for each gas; its *fingerprint* [6]. Therefore to sense a certain gas, it is necessary to measure the absorption at some of its specific wavelengths. That imposes isolating the absorption line, which can be accomplished with a high Q-factor PhC filter. The main drawback of such method is that to have good sensitivities, long interaction lengths must be attained.

An alternative to the previous methods was reported in other studies [7]–[9]. In them, it is proposed the use of the slow group velocities that the band structure of carefully crafted macroporous silicon (MPS) PhCs have at the band edges of the PBG. Theoretically this method was shown to work well, but light coupling was shown to be a major problem. Furthermore, losses due to scattering and absorption were also very high as the signal had to traverse a very long silicon structure.

In this paper we study a 3d MPS structure as proposed elsewhere [4], [10] for gas sensing, using out-of-plane (vertical) propagation. Although these PhCs are more complex, they can be fabricated using cheap methods, such as electrochemical etching (EE), and are very versatile structures. Furthermore, light coupling into and out of the sample is simpler than for in-plane devices. Additionally, MPS can be made to be inert to ambient conditions and aggressive gases, and are mechanically very stable.

The MPS PhC device analyzed in this paper has a modulated profile, and would be fabricated by EE. The proposed structure has a cavity to induce a resonance state which has been engineered to correspond with the absorption band of CO_2 at $\lambda = 4.25\,\mu$m. This device works as a filter to be placed in the optical path with an embedded resonator that introduces a narrow passband in the transmission spectrum to select the CO_2 absorption band and to discard other wavelengths. In order to optimize the optical response, the number of periods used in the modulated part of the PhC is changed from a few periods to a large number of them. Besides, as the PhC structure is a membrane to allow the passage of gas through its pores, the mechanical resilience has to be considered. As these membranes are very thin, porosification is continued after the 3d part of PhC is finished, consisting of straight pores. This section forms the *tail* of the pores. This is done in the same fabrication step and results in a thicker and robust device. This tail may result in unwanted optical features, and therefore the effect of its length is studied. The tail length is changed from non-existent to about the double of the PhC depth, to determine its impact or possible benefits to the optical transmittance of the proposed device. These proposed photonic crystals have been experimentally fabricated, showing a good accordance with the theoretical study. Although the experimental Q-factors are lower than the theoretical ones (due to non-idealities in the fabricated design), we report an enhancement of almost an order of magnitude in the quality factor of the peak. This achievement show that the new structures are a

promising option to be used in spectroscopic gas sensing. Finally, an improvement of the sensitivity due to the increase in the peak's quality factor is theoretically predicted.

2. NUMERICAL STUDY

The simulations of the 3d photonic crystals were done in Optiwave's OptiFDTD software, which uses the finite-difference time-domain method (FDTD). For the simulations, a single pore was designed with its axis aligned to the Z axis, and with light propagating along the Z axis. Periodic boundary conditions were applied on the *XZ* and *YZ* walls while perfect absorbing layers were used for the top and bottom of the simulation space in order to model an ideal PhC. The base shape of this pore consisted in two main parts: the modulated areas and the defect. Modulations were done by an number of periods composed, each one of them, by an ellipsoid and a cylinder—whose radius were optimized in our previous works [10].—Simulations dimensions were normalized to the lattice XY periodicity and each modulation period was defined in a normalized cell box of size 1×1×1 units. The defect, embedded halfway the pore depth, was introduced by removing a period, keeping a constant radius and extending as needed its length. For a real device, the lattice period would be $p_{\text{lattice}} = 0.7\,\mu$m in order to make the bandgap and defect state correspond with the carbon dioxide absorption line at $\lambda = 4.25\,\mu$m. It should be taken into account that the profile obtained experimentally shows certain variability compared to the designed one. As it can be seen in Fig. 1 (b), these variations are small and have little impact on the bandgap, as reported in [11]. However, small variations in the length of the defect can lead to a mismatch with respect to the working frequency for which it was designed. However, the position of the peak within the bandgap can be easily adjusted in few iterations in fabrication [11].

The quality factor of the cavity is calculated using the usual definition as $Q = f_{\text{peak}}/\text{FWHM}$ from the spectral data, where f_{peak} is the central frequency of the resonant state, and FWHM is the width of the peak at half of its maximum value. In order to achieve the strongest resonance and the highest Q-factor in transmission, and enhance the optical features of the photonic crystal, two modifications of the initial structure were performed. The first one was to introduce a region of porous silicon with a straight profile—i.e. with a constant radius—as a continuation of the modulated pores, that is a *tail* of the pores. The second was to increase the number of periods. All the simulated structures are permeable membranes, both pore ends open allowing the passage of gas. The studied morphologies are schematically depicted in Fig. 1.

The illumination was done with a plane wave coming from the top of the pore and impinging on the front face of the PhC. The light wave was a Gaussian pulse with a linewidth of $\Delta = 4\,\mu$m and a central wavelength about 5 μm, so to make it correspond to the CO_2 absorption line. The transmission spectrum was obtained by placing a plane detector 5 μm after the pore end. The spectrum was calculated by integrating the power flux through the detector plane and normalizing to the incident wave.

To perform the simulations, the refractive index of the bulk material was set to $n \approx 3.43$, which corresponds with the value of silicon in the range of $4\,\mu$m to $4.4\,\mu$m at room temperature [12]. As reported in previous

works [13], the absorption in low doped silicon has almost no effect in the propagation of light through the PhC. So, in consequence, no losses were introduced in the bulk material (imaginary part of its refractive index, $\kappa = 0$). The pores were filled initially with air. The structure optimization was performed under these conditions. After optimization, the air was changed with carbon dioxide, which has strong absorption in the MIR. In particular the wavelength $\lambda = 4.25\,\mu$m was selected because is the strongest absorption band of CO_2 and MPS sensing devices have already been reported [4]. The data of the absorption coefficient were obtained from HITRAN database at standard conditions[14]. The absorption coefficient and the imaginary permittivity of the gas are related by $\varepsilon_{im} = n(\omega) \cdot \alpha(\omega)/\omega$, [15, Ch. 3] where ε_{im} is the imaginary part of the permittivity, n is the refractive index, α is the absorption coefficient and ω is the angular frequency. For the purposes of this study, we have determined that the HITRAN data can be approximated by the fitting of two Drude-Lorentz oscillators [15] to the envelope of the absorption lines. At atmospheric pressures, the absorption lines will experience some broadening (HITRAN data is recorded in very low pressure conditions and high resolution) which can be seen in FTIR measurements. Furthermore, the resonance peak is designed to select the $4.18\,\mu$m to $4.25\,\mu$m wavelength range, which as shown in in Fig. 2, corresponds accurately to the DL model used.

2. EXPERIMENTAL

Preparation of macroporous silicon PhC with defect

The 3d structures were obtained by electrochemical etching of *n*-type ⟨1 0 0⟩ crystalline silicon samples in hydrofluoric (HF) acid solution. The starting material had a resistivity between 0.1-0.3 Ω·cm. An N^+ layer was implanted on the backside of the wafer to provide a low-resistance transparent ohmic contact. Next, the wafer was oxidized and a lithography of 700 nm pitch was performed. A Reactive-ion Etching (RIE) and a tetramethylammonium hydroxide (TMAH) etching were done to create inverted pyramid-shaped pits that will act as nucleation centers for the ordered pore growth. Finally, an electrochemical etching was done to control the modulation of pore diameter which, in its turn, is regulated by the applied current. This method allows to design the profile beforehand and to create smooth 3d structures of great complexity. In particular, the periodical profiles attached in Fig.7 a) have been generated. As depicted in the figure, a planar defect is introduced halfway the total pore depth by suppressing one of the modulations and leaving a constant diameter section. The length of the cavity is 1.7 μm with a width value of 0.23 μm in all the samples. Finally, the longest value achieved for the tail's length is 6.5 μm. The total depth of all samples was about 12 μm in the case of $N = 5$ and about 17 μm when $N = 8$. A complete description of the process can be found elsewhere [16].

The optical response of the fabricated samples was measured in the MIR range using a Bruker Optic's Vertex FT-IR spectrometer. The lattice was aligned to the Γ – M direction (along one lattice axis in the surface) and an aperture of 1 mm and a resolution of 4 cm^{-1} was used. The measurements have been referred to the source spectrum to normalize the results in both, reflectance and transmittance.

3. RESULTS AND DISCUSSIONS

Creating a PhC membrane as short as the initially proposed, is a challenge in fabrication difficult to overcome. Lengthening the pores with a straight part at the end—see Fig. 1 (b)—is a good solution that allows to have longer pores as well as the optical properties of the photonic crystals are preserved. Furthermore, this added tail can be used to enhance the transmitted peak features. In classical optical filters, $\lambda/4$ cavities are used to optimize the coupling between dissimilar refractive index media at the working frequency, which is adjusted by setting the cavity's length. Therefore, it seems beneficial to place a $\lambda/4$ tail at the end of the pore to enhance coupling and hence the Q-factor of the main peak. Nevertheless, as reported in Geppert's thesis [7], the coupling behavior in photonic crystals cannot be explained classically; resonant conditions and Bloch's modes have to be considered for designing the tail's length in order to optimize the peak's features.

According to Geppert's study, simulations show that additional resonant modes appear in the bandgap as the length of the tail is increased. This further modifies the shape of the main peak, and thus its Q-factor. In Fig. 3 it is depicted the influence in the peak's shape when the length of tail of the pores was varied from $0\,\mu$m to $40\,\mu$m while the rest of the parameters—porosity, periodicity, and modulation profile—remained unchanged, since they were optimized in previous works[13]. Adjusting the tail's length and diameter, the number and position of the resonances in the tail section change accordingly. As expected, the longer the tail, more modes will exist. These can be wisely placed, by carefully adjusting the tail's length, such that these resonant peaks narrow the defect state. As seen from Fig. 3, the optical transmittance for different tail sections shows almost no change in amplitude. Therefore, in the optimum case, the Q-factor of the defect's resonance improves. The trade-off is the rise of ground level in the PBG. The adjustment of the geometry can also be sensitive to process variations, as small variations can result in the loss of performance.

In the data shown in Fig. 3 (d) it can be observed how the main resonance peak splits in two peaks. This can be explained as, for lengths greater than $24\,\mu$m, the resonant peaks given by the tail's length appear so close one to each other that at least two of them fall in the main peak, splitting it in two. As the length of the tail increases, this suggests that more peaks may fall over the defect resonance. However, fabrication imperfections ultimately break coherence [17] and the tail won't have any significant contribution to the optical response of the PhC. As reported in Koenderink's work [17], the total length of the PhC should not exceed some tens of times the lattice parameter to preserve the optical properties. Taking into account both constraints—length of the PhC and the emergence of two peaks,—it seems reasonable to restrict the tail's length to the range of $0\,\mu$m to $20\,\mu$m.

Another important fact observed in these simulations is that as we increase the tail's length l_{tail}, the Q-factor is also increased. In particular, the Q-factor achieved with no tail is $Q = 127$, but increases to $Q = 215$ when $l_{\text{tail}} = 20\,\mu$m. This amount allows to measure the gas concentration by the dispersive method, based in Beer-Lambert's formula[6]. The greatest sensitivity is given when the strongest absorption line of CO_2 and the cavity resonance of the PhC are aligned. In Fig. 4, it can be observed that the variation between the curves of 0% and 100% of concentration is almost the 20% of the amplitude for the initial structure.

Previous studies have reported the impact that the number of layers *N* have in the transmission spectra in PhCs [18]–[21]. They prove that the bandgap becomes more defined as the number of periods increase. Furthermore, in the case of having a transmission peak in the gap, it can be shown that both, Q-factor and amplitude, are related with the quantity of periods [22]. According to this, we increased the number of periods before and after the defect respect to the base case, see Fig. 1 (c). As depicted in Fig. 5, increasing the number of periods *N*, rises significantly the Q-factor of the peak. However, as a counterpart, the amplitude decreases. As shown in Fig. 6 (b), a convenient compromise between the quality factor and the transmission is reached when the number of periods is around nine, showing a Q-factor close to 500 and a transmission of 66%. These values improve the results obtained just by adding a tail to the pores.

The effect of the presence of CO_2 in these optimum conditions can be seen in Fig. 6 (a) for different gas concentrations. The amplitude of the peak has a greater change when exposed from 0% to 100% of gas concentrations than for the initial device of Fig. 4

If both strategies for enhancing the peak characteristics –e.g. lengthening the pore and increasing the number of periods- are applied together, the previous results are improved to the highest Q-factor of $Q = 902$ when $N = 9$ and $l = 20$ μm.

These theoretical results obtained through simulation have been experimentally tested. In Fig. 7a) it is depicted the transmission spectra for the studied cases. The profiles with five and eight periods are shown in Fig. 7b). Due to experimental limitations, the tail length has only been able to reach 6.5 μm in both periodicities, being far from the optimal value discussed above (20 μm). In the same sense, the number of periodicities have been limited to N = 8 because adding more periods significantly reduced the transmittance. Even so, by introducing a tail to the profile of five modulations, the Q-factor shows a remarkable improvement, going from Q = 12 (case without tail) to Q = 61. A larger increase is obtained when more periods are introduced, reaching the value of Q = 101. But it is when both strategies are applied at the same time when the best quality factor is obtained, Q = 117, almost an order of magnitude higher than the initial value.

Although experimental values are not as good as the theoretical ones (due to non-idealities in fabrication, e.g. small variations in pore length or thickness, roughness, etc.), they do support the developed analytic study. Moreover, thanks to the improvement of Q-factor, experimental peaks have been obtained good enough to perform gas spectroscopic measurements with them (see Fig. 4 where a peak of Q ≈ 120 has been used in the simulation). However, as Figure 8 shows, an improvement in the Q-factor would revert to a greater sensitivity of the device.

In Fig. 8(a) it is depicted the amplitude of the transmission peak relative to the concentration of carbon dioxide inside the pores in three cases, N = 5, 7 and 9 for $l = 20\ \mu$m in all of them. Increasing the number of periods, *N*, reduces the light leakage through the PBG of the photonic crystal. This enhances the time the light interacts with the gas inside the defect, thus enlarging the effective path length of the defect (by the Q-factor). This effect is demonstrating looking at the sensitivity $S = \partial I_t / \partial C_{gas}$, plotted in Fig. 8(b).

4. CONCLUSIONS

In this paper 3d PhC based on MpS have been studied by simulation. The crystal's shape has been explored to find an optimum Q-factor of a photonic filter based on 3d MpS where light propagates along the pore's axis. The considered PhC structure in this analysis is a square array of modulated pores with an embedded plane defect that gives rise to a photonic bandgap and a transmission peak in the middle of the PBG. The shape optimization involved adjusting the pores' tail length and modifying the number of periods in the modulated section.

It has been found that the presence of a tail section of straight pores after the modulated PhC can have a noticeable effect for a certain length of this tail. In particular, the simulations show that, at wavelengths around $\lambda = 4\,\mu$m, for tails lengths up to about $20\,\mu$m several small resonance peaks appear due to resonance in the tail, which can have a positive effect in the main resonance peak due to the plane defect. This allows increasing the Q-factor without affecting appreciably the transmitted maximum. However, for tails longer than $20\,\mu$m, these secondary resonances start interfering with the main peak which can result in a loss of performance. The presence of this tail is necessary when fabricating porous membranes to provide mechanical resilience to the device. Typically, this tail has a length about $70\,\mu$m or longer. It has been found that for such long tails [17], and due to fabrication roughness backside, these secondary resonances are virtually non-existent and can be neglected.

On the other hand, the number of periods of the modulated crystal has a greater impact on the Q-factor. Generally, increasing the number of periods will give a higher Q-factor for the resonant cavity. Nonetheless, there exists a tradeoff with the transmitted peak amplitude. As the period number increases, the peak amplitude decreases. The optimum number will therefore depend on the source intensity, the detector sensitivity and the noise floor, but from the performed study we find that using nine modulation periods both before and after the defect gives a very good compromise.

These new structures have been studied, supporting the developed theory. In concrete, the initial value of the Q-factor for the basic case ($N = 5$, without tail), have been increased up to $Q = 117$, in the case of having a photonic crystal with 8 periods in each modulation area and a tail of 6.5 microns. This new optical features are thus promising to be applied in spectroscopic gas sensing.

Finally, the device response to CO_2 has been studied. It has been found that for the optimized PhC structure, a large variation of 70% in transmitted peak amplitude can be obtained with a sensitivity of about 0.8, relative variation of the transmission amplitude respect to gas concentration. Therefore we conclude that such PhCs are suitable for the detection of strong absorbing gases by non-dispersive infrared spectroscopy.

5. ACKNOWLEDGEMENT

This work has been funded by the Spanish Ministerio de Economía y Competitividad (MINECO) through grant TEC-2013-48-147-C6-2

The authors would like to thank P. Eglitis for his helpful comments during the preparation of this paper.

REFERENCES

[1] J. N. Winn, Y. Fink, S. Fan, and J. D. Joannopoulos, "Omnidirectional reflection from a one-dimensional photonic crystal.," *Opt. Lett.*, vol. 23, no. 20, pp. 1573–1575, 1998.

[2] H. Xu, P. Wu, C. Zhu, A. Elbaz, and Z. Z. Gu, "Photonic crystal for gas sensing," *J. Mater. Chem. C*, vol. 1, no. 38, p. 6087, Sep. 2013.

[3] A. Zakrzewski, M. Wielichowski, and S. Patela, "Optimization of 2D slab photonic crystal geometry for gas sensing," in *2011 International Students and Young Scientists Workshop "Photonics and Microsystems,"* 2011, pp. 147–149.

[4] D. Vega, F. Marti, A. Rodriguez, and T. Trifonov, "Macroporous silicon for spectroscopic CO_2 detection," in *IEEE SENSORS 2014 Proceedings*, 2014, pp. 1061–1064.

[5] H. Ren, J. Zhang, Y. Qin, K. Liu, Z. Wu, W. Hu, C. Jiang, and Y. Jin, "Ring resonator of surface modes based on photonic crystals," *Opt. Commun.*, vol. 284, no. 16–17, pp. 4073–4077, Aug. 2011.

[6] J. Hodgkinson and R. P. Tatam, "Optical gas sensing: a review," *Meas. Sci. Technol.*, vol. 24, no. 1, p. 12004, Jan. 2013.

[7] T. M. Geppert, "Towards Photonic Crystal-Based Spectroscopic Gas Sensors," Thesis, Hälle-Wittenberg, 2006.

[8] R. B. Wehrspohn, S. L. Schweizer, B. Gesemann, D. Pergande, T. M. Geppert, S. Moretton, and A. Lambrecht, "Macroporous silicon and its application in sensing," *Comptes Rendus Chim.*, vol. 16, no. 1, pp. 51–58, 2013.

[9] A. Lambrecht, S. Hartwig, S. L. Schweizer, and R. B. Wehrspohn, "Miniature infrared gas sensors using photonic crystals," 2007, p. 64800D.

[10] D. Vega, D. Cardador, M. Garín, T. Trifonov, and A. Rodríguez, "The Effect of Absorption Losses on the Optical Behaviour of Macroporous Silicon Photonic Crystal Selective Filters," *J. Light. Technol. Vol. 34, Issue 4, pp. 1281-1287*, vol. 34, no. 4, pp. 1281–1287, 2016.

[11] D. Cardador, D. Vega, D. Segura, and A. Rodríguez, "Study of resonant modes in a 700nm pitch macroporous silicon photonic crystal," *Infrared Phys. Technol.*, vol. 80, pp. 6–10, Jan. 2017.

[12] B. J. Frey, D. B. Leviton, and T. J. Madison, "Temperature-dependent refractive index of silicon and germanium," in *SPIE Astronomical Telescopes + Instrumentation*, 2006, p. 62732J–62732J–10.

[13] D. Vega, D. Cardador Maza, T. Trifonov, M. Garin Escriva, and A. Rodriquez Martinez, "The Effect of Absorption Losses on the Optical Behaviour of Macroporous Silicon Photonic Crystal Selective Filters," *J. Light. Technol.*, vol. 34, no. 4, pp. 1281–1287, 2015.

[14] L. S. Rothman, I. E. Gordon, A. Barbe, D. C. Benner, P. F. Bernath, M. Birk, V. Boudon, L. R. Brown, A. Campargue, J.-P. Champion, K. Chance, L. H. Coudert, V. Dana, V. M. Devi, S. Fally, J.-M. Flaud, R. R. Gamache, A. Goldman, D. Jacquemart, I. Kleiner, N. Lacome, W. J. Lafferty, J.-Y. Mandin, S. T. Massie, S. N. Mikhailenko, C. E. Miller, N. Moazzen-Ahmadi, O. V. Naumenko, A. V. Nikitin, J. Orphal, V. I. Perevalov, A. Perrin, A. Predoi-Cross, C. P. Rinsland, M. Rotger, M. Šimečková, M. A. H. Smith, K. Sung, S. A. Tashkun, J. Tennyson, R. A. Toth, A. C. Vandaele, and J. Vander Auwera, "The HITRAN 2008 molecular spectroscopic database," *J. Quant. Spectrosc. Radiat. Transf.*, vol. 110, no. 9–10, pp. 533–572, Jun. 2009.

[15] F. Wooten, *Optical Properties of Solids*. Academic Press, 1972.

[16] V. Lehmann, "The Physics of Macropore Formation in Low Doped n-Type Silicon," *J. Electrochem. Soc.*, vol. 140, no. 10, p. 2836, Oct. 1993.

[17] A. F. Koenderink, A. Lagendijk, and W. L. Vos, "Optical extinction due to intrinsic structural variations of photonic crystals," *Phys. Rev. B*, vol. 72, no. 15, p. 153102, Oct. 2005.

[18] J. F. Bertone, P. Jiang, K. S. Hwang, D. M. Mittleman, and V. L. Colvin, "Thickness Dependence of the Optical Properties

of Ordered Silica-Air and Air-Polymer Photonic Crystals," *Phys. Rev. Lett.*, vol. 83, no. 2, pp. 300–303, Jul. 1999.

[19] H. S. Lee, R. Kubrin, R. Zierold, A. Y. Petrov, K. Nielsch, G. A. Schneider, and M. Eich, "Thermal radiation transmission and reflection properties of ceramic 3D photonic crystals," *J. Opt. Soc. Am. B*, vol. 29, no. 3, p. 450, Feb. 2012.

[20] E. Moreno, F. J. García-Vidal, and L. Martín-Moreno, "Enhanced transmission and beaming of light via photonic crystal surface modes," *Phys. Rev. B*, vol. 69, no. 12, p. 121402, Mar. 2004.

[21] C.-J. Wu and Z.-H. Wang, "PROPERTIES OF DEFECT MODES IN ONE-DIMENSIONAL PHOTONIC CRYSTALS," *Prog. Electromagn. Res.*, vol. 103, pp. 169–184, 2010.

[22] X. Xiao, W. Wenjun, L. Shuhong, Z. Wanquan, Z. Dong, D. Qianqian, G. Xuexi, and Z. Bingyuan, "Investigation of defect modes with Al2O3 and TiO2 in one-dimensional photonic crystals," *Opt. - Int. J. Light Electron Opt.*, vol. 127, no. 1, pp. 135–138, Jan. 2016.

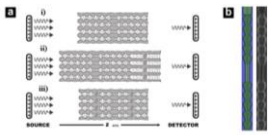

Fig. 1. (a) Schematic representation of the different structure variations. A broadband light impinges the sample and travels through the photonic crystal (i) the basic structure consists of two modulated areas separated by a cavity in the middle. (ii) The modulated pores have been extended with a length of constant diameter pores. (iii) The number of periods before and after the defect is changed. As shown, light propagates along the Z axis, i.e. aligned to the pores' axis. (b) Comparison of simulated and etched basic profiles.

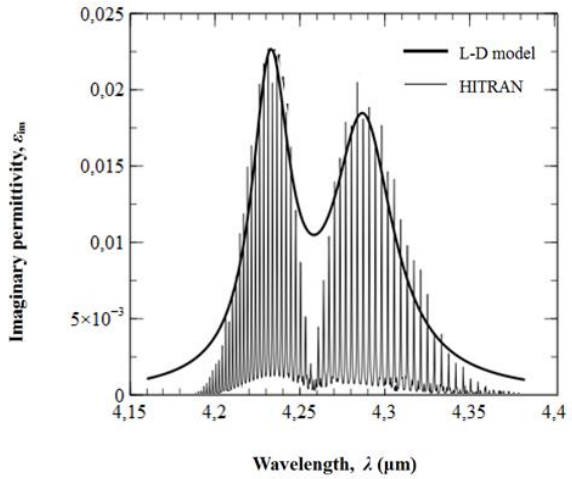

Fig. 2. Absorption lines for CO_2 and the Lorentz-Drude approximation used in this paper which consists on modeling the gas absorption as the envelope (dark) of his absorption lines (grey).

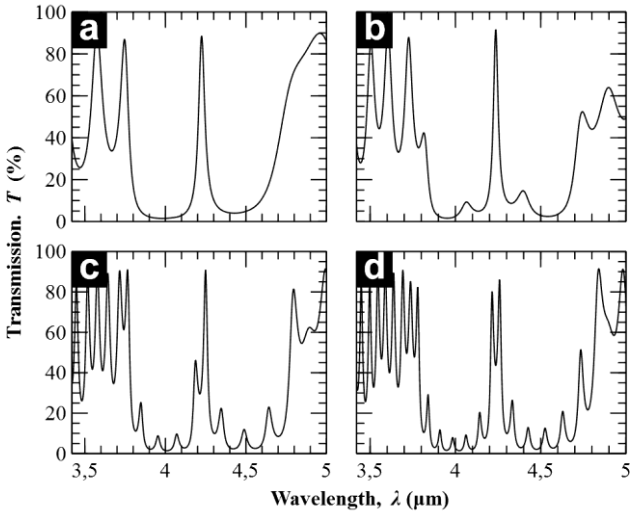

Fig. 3 Keeping the number of periods constant, the straight end section length is varied. As the length increases, new, smaller, peaks appear in the optical spectrum. Here are shown the optical response of the PhC with defect when the tail is (a) 0, (b) 10, (c) 26, and (d) 40 μm long.

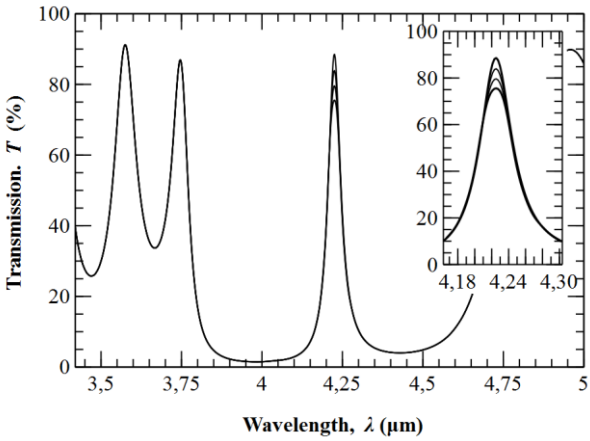

Fig. 4. Evolution of peak's amplitude for the base PhC with a when exposed to 0%, 33%, 66% and 100% of gas concentration.

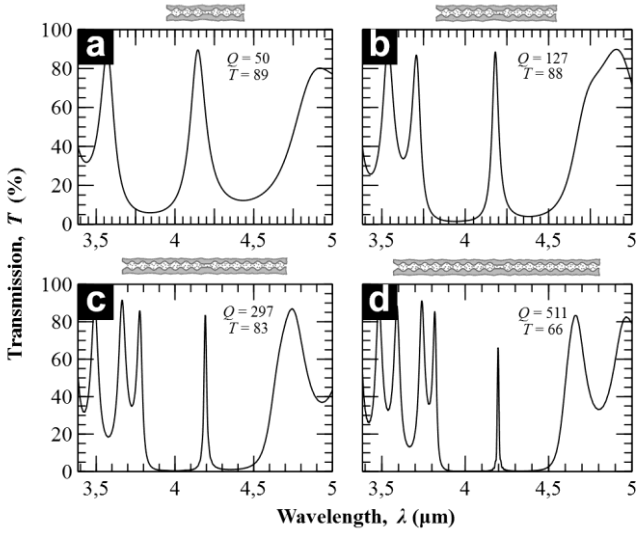

Fig. 5. Evolution of the amplitude and the Q-factor with respect ot the number of periods: (a) 3 periods, (b) 5 periods, (c) 7 periods, and (d) 9 periods. The actual strucrtures are depicted above the graphs for each case.

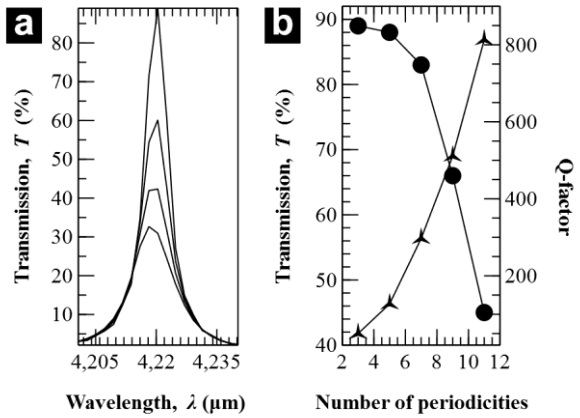

Fig. 6. Detail of the peak amplitude change with gas concentration. The MPS device has 9 modulation periods and a tail section of length $l = 20\,\mu$m. In (a) the peak amplitude clearly decreases for CO_2 concentration of 0%, 33%, 66%, and 100%. In (b) the peak's amplitude (●) and Q-factor (⅄) dependence to the number of periods is plotted.

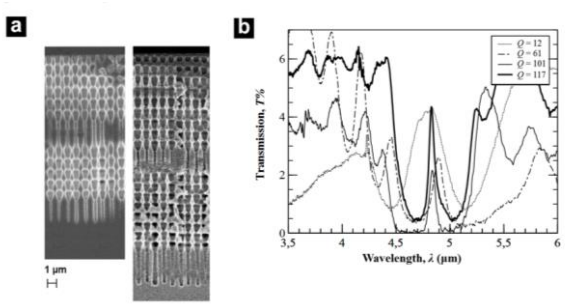

Fig. 7. (a) Scanning electron microscope (SEM) image of two photonic crystals with N = 5 and 8, respectively. The tail has been lengthened until 6.5 μm in both cases. (b) Transmission spectra of the structures with and without tail: N = 5 and L = 0 μm (dotted line), N = 5 and L = 6.5 μm (dot-dashed line), N = 8 and L = 0 μm (light-black line), N = 8 and L = 6.5 μm (dark-black line).

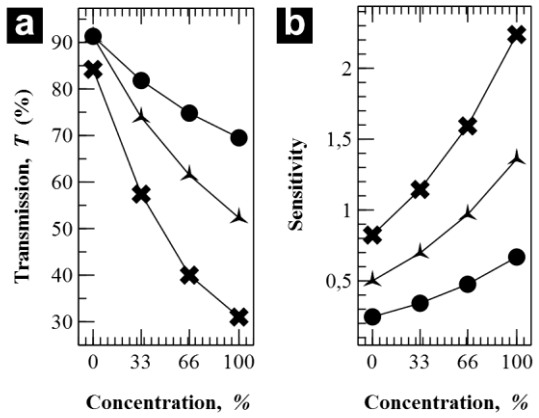

Fig. 8. (a) Evolution of the peak's amplitude when exposed to 0%, 33%, 66% and 100% of gas concentration in for the number of periodicities N (●) 5, (×) 7, and (⅄) 9. In all cases l = 20 μm. (b) Sensitivity in the three cases.